A01-34121

# AIAA 2001–3339

## Enhancement of Electrodynamic Tether Electron Current Collection Using Radio Frequency Power: Numerical Modeling and Measurements

Éric Choinière and Brian E. Gilchrist
*University of Michigan, Ann Arbor, Michigan 48109*
Sven G. Bilén
*The Pennsylvania State University, University Park, Pennsylvania 16802*

**37th AIAA/ASME/SAE/ASEE Joint Propulsion Conference and Exhibit**
8–11 July 2001
Salt Lake City, Utah

# Enhancement of Electrodynamic Tether Electron Current Collection Using Radio Frequency Power: Numerical Modeling and Measurements

Éric Choinière* and Brian E. Gilchrist†
*University of Michigan, Ann Arbor, Michigan 48109*
Sven G. Bilén‡
*The Pennsylvania State University, University Park, Pennsylvania 16802*

**Tether electron current collection in the Orbital Motion Limited regime is one of the limiting factors in power and thrust generation applications of electrodynamic tethers. Injection of radio frequency power along tethers is considered in order to enhance electron current collection. As a basic assessment tool, Particle-In-Cell modeling of the tether system is performed using a 1-d cylindrical code. Comparison of test electron trajectories shows that the time periodic field distribution created by the RF excitation results in electrons being scattered off their usual OML trajectories, which under some conditions increases their probability of being collected by the tether. Analysis of simulation results reveals that large current enhancements can occur at resonance frequencies of the input reactance (where $X_{\text{in}} = 0$), but at the expense of high RF power. Current enhancement is best measured in terms of the relative current variation per unit of RF power dissipated for every 1-meter section of the tether. Optimum enhancements of about 9% per RF watt per meter were obtained by simulation at low frequencies (75 MHz). Similar enhancements were observed during Phase 1 of the experimental measurements on tether samples. Initial experimental results from Phase 2 of the tests are presented in which the RF power was kept constant at a reference plane along the transmission line connecting to a tether sample. These results show some frequency dependence of the current enhancement for a fixed power level. Further measurements are needed which will control the RF power sent at the tether sample itself, rather than at an upstream position on the transmission line.**

## Nomenclature

| | |
|---|---|
| $e$ | electron charge (C) |
| $f_{pe}$ | electron plasma frequency (Hz) |
| $f_{pi}$ | ion plasma frequency (Hz) |
| $\Gamma$ | power reflection coefficient at the probe |
| $I_{\text{dc}}$ | average collection current (A) |
| $I_{\text{dc0}}$ | measured DC current without an RF signal (A) |
| $I_{\text{oml}}$ | collection current predicted by OML theory (A) |
| $l$ | length of the tether sample (m) |
| $m_e$ | electron mass (kg) |
| $n_e$ | electron plasma density ($\text{m}^{-3}$) |
| OML | Orbital Motion Limit |
| PIC | Particle-In-Cell |
| $P_{\text{coupler}}$ | net RF power at the coupler output (W) |
| $P_{\text{in}}$ | incident RF power (W) |
| $P_{\text{out}}$ | reflected RF power (W) |
| $P_{\text{probe}}$ | net RF power at the probe (W) |
| $r_a$ | radius of the tether sample (m) |
| $r$ | radial distance measured from the center of the tether conductor (m) |
| $r_1$ | radius of simulated outer conductor (m) |
| $t$ | time elapsed, measured from the instant a test particle is released (s) |
| $T_e$ | electron temperature (eV) |
| $V_{\text{ac}}$ | AC applied voltage (V) |
| $V_{\text{dc}}$ | DC applied voltage (V) |
| $V_p$ | probe voltage (V) |

## Introduction

BARE electrodynamic space tethers are under consideration for applications such as power and thrust generation for orbiting spacecraft. In these applications, one of the primary concerns is the ability of the system to collect electrons from the surrounding ionospheric plasma in order to maximize the amount of electrical power or thrust provided. For a positive value of the applied DC potential with respect to the surrounding plasma, the amount of electrical power or thrust provided increases with the magnitude of the current flowing on the tether, which in turn is limited

*Graduate Student, Radiation Laboratory, EECS Department
†Associate Professor, Electrical Engineering and Space Sciences, AIAA Senior Member
‡Assistant Professor, Communications and Space Sciences Laboratory, AIAA Member

by the tether's ability to collect electrons from the surrounding plasma.

Under certain conditions, the current collected by a positively biased long circular cylinder such as a tether immersed in a low-density plasma can be described by the Orbital Motion Limited (OML) current law:

$$I_{\mathrm{oml}} = 2r_a l n_e e \sqrt{2eV_p/m_e} \ , \qquad (1)$$

which is based on conservation of angular momentum.[1] This relationship is valid provided that the applied voltage is large compared to the electron temperature and that the tether radius is small compared to the plasma Debye length. Thus, it is seen that the amount of current collected per unit length of the tether is controlled by the magnitude of the applied voltage and the radius of the tether.

In order to *increase the electron current collection beyond the apparent limitation described above,* a technique is proposed here that consists of the injection of a radio frequency signal superposed on the bias potential and propagated along the transmission line formed by the tether sheath structure.[2] Analogous to the resonance condition on spherical probes observed by Lepechinsky[3] and others, a resonance condition on the tether sheath structure was experimentally observed on a long cylindrical probe, which occurred at a frequency slightly under the electron plasma frequency. These experiments consisted in applying a 15-V rms sinusoid voltage onto a bare 10-cm long tungsten tether sample biased at 140 V DC. The simulated tether was immersed in a Xenon plasma at a density of $10^{14}$ m$^{-3}$. Results indicated that a large increase in the collected current occurred over a narrow frequency band centered at a frequency slightly under the electron plasma frequency.

In this paper, we will present the Particle-In-Cell model that was used to model the enhancement phenomenon, describe the basic physics underlying the possible current enhancement, and finally describe the simulation results as well as the experimental data that was collected on two occasions, which we refer to as "Phase 1" and "Phase 2".

## Particle-in-Cell Model and Issues

The particle-in-cell (PIC) technique was used in order to model the tether–plasma interactions and characterize the enhancement phenomenon that previously was observed experimentally. A 1-dimensional cylindrical implementation of the PIC technique[4] was adapted and used to this end. The analysis of the simplified problem is based on assumptions of a collisionless plasma, a negligible plasma drift velocity, quasi-static electromagnetic fields, and no external magnetic field. Another important assumption concerns the ion density distribution, which is assumed to be uniform everywhere around the tether; this is the well-known *matrix sheath* approximation[5,6] and is valid when $f \gg f_{pi}$.

Fig. 1 depicts the geometry of our simplified model. An outer perfect electric conductor at $r = r_1$ is used as the boundary condition representing the plasma potential reference, arbitrarily set to zero here. The potential difference between the center and outer conductor is set to a sinusoidal potential variation of amplitude $V_{\mathrm{ac}}$ on top of a bias potential $V_{\mathrm{dc}}$. It should be noted that the `xpdc1` computer code[4] has been modified such that the number of electrons present in the simulation domain remains constant during the simulation. For this purpose, for every electron collected either on the tether or on the outer conductor, another electron is emitted from the outer conductor with its three velocity components chosen according to a Maxwellian distribution at the bulk plasma electron temperature. As a consequence, the plasma potential is kept constant and very close to zero.

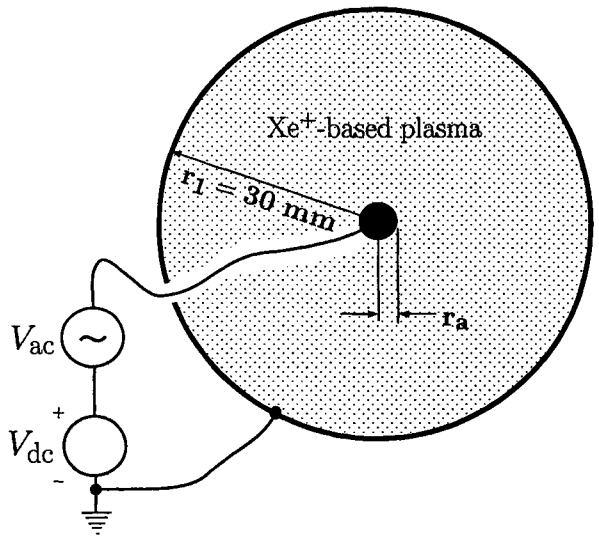


**Fig. 1 Basic geometry of the simplified model of the electrodynamic tether problem.**

Because of memory and computing power limitations, each individual electron cannot be included in the simulations. Instead, a reduced number of particles with larger charge and mass are simulated. The ratios used for the number of real electrons to the number of simulated particles were in the range of $10^7$ to $10^8$. In order to compensate for noise in the simulation diagnostics caused by the artificial granularity of the simulation, results were averaged over many RF cycles after an initial delay. Many diagnostics were computed using this averaging technique, among which are the average collected DC current ($I_{\mathrm{dc}}$), average sheath width, the fundamental and harmonics of the time-varying current response, the average RF power dissipated in the sheath, the input impedance, and the steady-state time-periodic electric field distribution.

## Basic Physics of the Enhancement Phenomenon

The known non-linear behavior of the plasma sheath surrounding the tether could be used to obtain an increased DC current with the application of a time-varying potential. An enhancement would be triggered by the time varying electric fields surrounding the tether, which scatter electrons off their OML trajectory by gradually increasing their radially directed velocity, resulting in more incoming electrons being collected on the tether.

From the PIC simulations, an evaluation of the steady-state time periodic electric field distribution (a function of $r$ and $t$) was obtained from averages over several RF cycles. This time periodic field is a solution that accounts for all electron plasma dynamics around the tether. Running a test particle (an electron) through this field-solution allows one to predict its trajectory as a function of initial position, velocity, and time of release with respect to the phase of the applied RF signal on the tether.

Fig. 2 shows the trajectories of two test electrons with identical initial conditions (thermal velocity corresponding to $T_e = 0.8$ eV and incident angle of 16.6 degrees off the horizontal) through both a DC potential distribution (no RF excitation on the tether) and an RF-enhanced potential distribution. For the case presented here, the initial angular momentum of the electron is too large compared to its radial velocity for it to be collected by the tether with the DC excitation alone. The RF enhancement, however, results in the scattering of the electron from the OML trajectory. In the illustrated case, the electron running through the RF-enhanced field is collected. The DC bias was 120 V in both cases and a 75-MHz, 10-V amplitude RF signal was added in the second case; the frequency used was lower than the electron plasma frequency of 152 MHz corresponding to an electron plasma density of $2.9 \times 10^{14}$ m$^{-3}$.

Although Fig. 2 illustrates a case where the electron running through the RF-enhanced field is collected, this is so only for a certain range of "release phases" measured with respect to the phase of the RF signal source. However, part of the electron population incoming at an incidence angle of 16.6 degrees with the same velocity will be collected, whereas none are in the DC case. An adverse effect is that some of the electrons that would normally be collected under DC conditions (at lower incidence angles, for example) might be scattered off the collection trajectory and be repelled. Although only the collective behavior formed by the combination of all scattered trajectories will determine whether electron collection is increased or decreased from the DC situation, this simple analysis illustrates how RF excitation might lead to current enhancement.

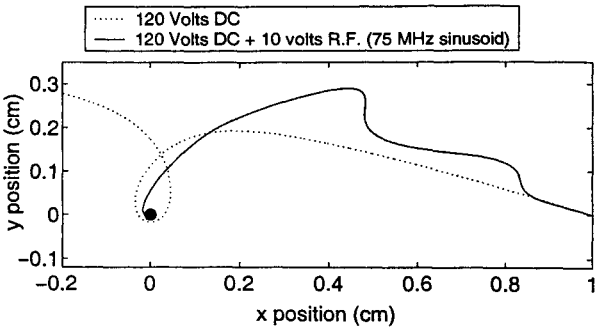


**Fig. 2 Trajectories of two test electrons through the steady-state, time-periodic potential distributions around a tether computed using a particle-in-cell code. Both test particles are incident at the thermal velocity (corresponding to $T_e = 0.8$ eV) and an incident angle of 16.6 degrees off the horizontal from the right-hand side. The first electron escapes (is not collected) while the second one, being scattered off the OML trajectory by RF oscillations, is collected.**

## Simulation and Experimental Results for Phase 1

The experimental measurements were performed at the Plasmadynamics and Electric Propulsion Laboratory (PEPL) at University of Michigan, in the Large Vacuum Test Facility (LVTF). In phase 1 of the tests, a 10-cm long cylindrical tether was immersed in a high-speed Xenon-based plasma generated by a Hall-effect thruster[7] developed at University of Michigan and the Air Force. Specific experiment parameters are listed in Table 1 and Fig. 3 illustrates the overall experimental configuration.

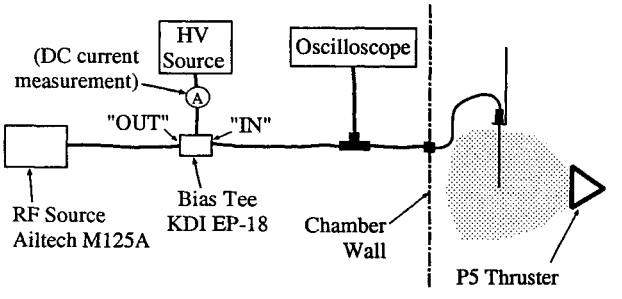


**Fig. 3 Experimental configuration for Phase 1 (Dec. 23, 1999)**

It should be noted that the value used here for $n_e$ was obtained by calibrating the model in order to fit the simulated and experimental resonances. This approximation agrees fairly well with that experimentally determined via Langmuir probe and resonance probe measurements. This experiment was performed along with an experiment that examined the DC current collection to bare cylinders in a high speed plasma flow, indicating that the probe used here was collecting in the OML regime with DC bias alone.[8,9] Also, all simulation results presented here were computed using

**Table 1 Parameters of interest for "Phase 1"**

| Parameter | Value |
|---|---|
| $n_e$ | $9.4 \times 10^{14}$ m$^{-3}$ |
| $r_a$ | 0.115 mm |
| $l$ | 10 cm |
| $V_{\rm dc}$ | 140 V |
| $V_{\rm ac}$ | 21.2 V (15 V rms) |
| $T_e$ | $\sim$ 1–2 eV |
| $f_{pe}$ | 275 MHz |
| $I_{\rm oml}$ | 24.2 mA |

the PIC technique with an nc2p (a parameter representing the number of actual particles to simulated particles) of $10^7$ and a time step $dt = 2.5 \times 10^{-11}$ s.

Figures 4 and 5 present a comparison of simulation and experimental results for the average collected current. Both responses show a resonance near 198 MHz, where an enhancement of electron collection is observed. In the experiment, an enhancement of approximately 750% was observed for the DC current. However, the levels of enhancement of simulated and experimental results cannot be compared, because the actual AC applied voltage on the tether could not be controlled with the experimental configuration that was used. The simulation results, which were realized under conditions of constant input AC voltage amplitude, show an enhancement of the order of 70% at the 198-MHz resonant frequency. Another major distinction between the simulations and measurements is the bandwidth of the enhancement, which was much smaller in the experiment than in the simulations.

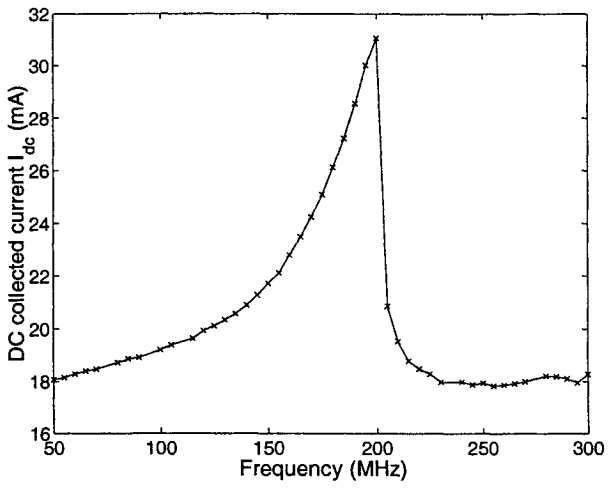


**Fig. 4 Simulated average collected current**

The enhancement effect of DC current is associated with an increase of the time-averaged sheath width (shown in Fig. 6). This increase near the resonance frequency of 198 MHz can be seen even though convergence of the curves has not been obtained due to computing time limitations. The enhancement of the average sheath signifies that the tether's electric field

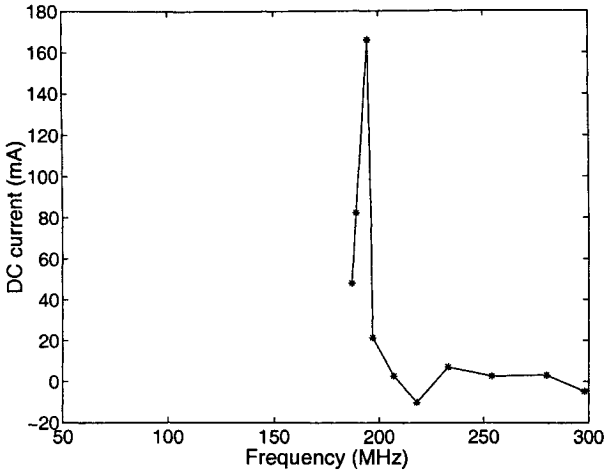


**Fig. 5 Measured average collected current**

reaches further out, allowing it to attract a larger number of electrons.

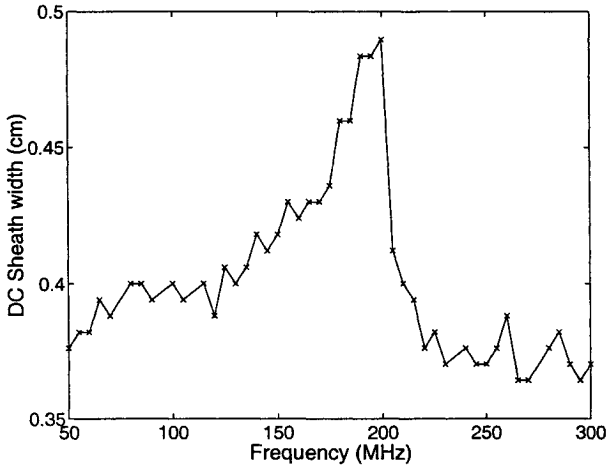


**Fig. 6 Simulated sheath width**

The resonance condition on the DC current collection comes about because the input reactance of the plasma-immersed tether crosses zero at $f = 198$ MHz, which results in a peak of the injected RF power (see Fig. 7) since we have an ideal voltage source. In our collisionless model, all RF power is transformed into radially-directed kinetic energy of the local electron plasma, which seems to be the fundamental mechanism leading to the increase of sheath size and the enhancement of electron collection.

Because the RF power level at the tether varies over frequency, simply comparing levels of DC current enhancement for a fixed RF voltage does not yield a useful figure-of-merit. As can be seen in Fig. 8, the DC current enhancement is proportional to the input RF power for a reasonably low range of power levels. Thus, a useful figure-of-merit would be the relative current enhancement per unit watt of RF power per meter; that is, the relative variation of DC current when 1 W of RF power is injected for every meter of

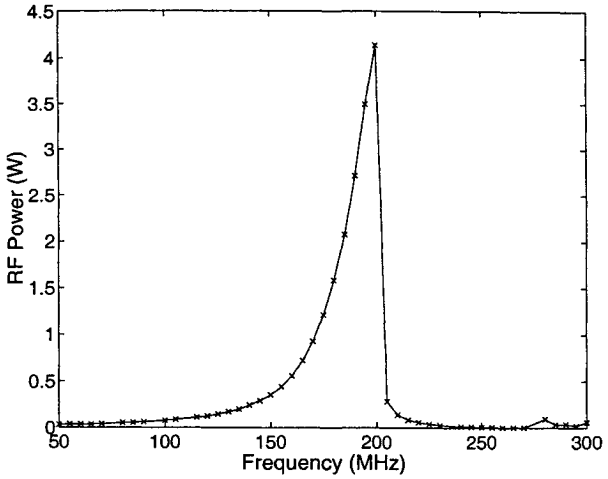


**Fig. 7 Simulated Injected RF power**

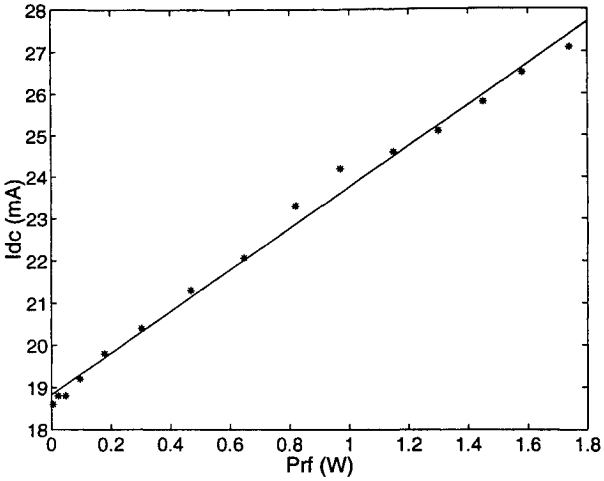


**Fig. 8 DC collected current vs input RF power (PIC simulation)**

tether. Fig. 9 depicts this figure-of-merit for the simulation results. Results are approximate, because the reference level for the DC current without RF excitation has been taken as the $f = 50$ MHz data, for which a small but non-zero RF power was injected. However, it can clearly be seen from the graph that the optimum current enhancement does not occur at the resonant frequency of 198 MHz, which actually presents a local minimum. The "lowest cost" of current enhancement occurs near $f = 90$ MHz, much lower than the resonant frequency; a current enhancement on the order of 9% is obtained for every watt of RF power injected per meter of tether length. This optimum frequency corresponds to a region of highly non-linear behavior; note that this peak occurs in spite of the low level of injected RF power at this frequency (Fig. 7). The sharp drop after $f = 220$ MHz in the relative current enhancement shown on Fig. 9 might explain the dip in the measurement occuring near the same frequency (Fig. 5), if one assumes that the injected RF power level was approximately constant during the experiment. This is expected since the input reactance (not shown) is nearly singular around 250 MHz.

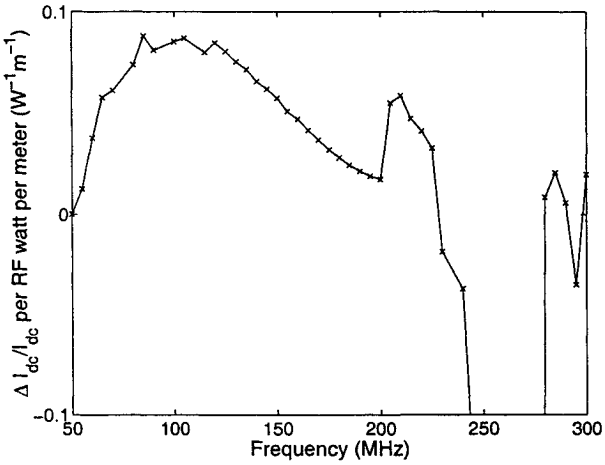


**Fig. 9 Relative variation of DC current per meter of tether per watt of RF power injected**

## Initial Experimental Results for Phase 2

In "Phase 2" of the tests, a 29.9-cm long cylindrical tether was immersed in the high-speed Xenon-based plasma discussed earlier. Table 2 lists the parameters of interest for these measurements.

**Table 2 Parameters of interest for "Phase 2"**

| Parameter | Value |
|---|---|
| $n_e$ | $9 \times 10^{14}$ m$^{-3}$ |
| $r_a$ | 0.140 mm |
| $l$ | 29.9 cm |
| $V_{\rm dc}$ | 100 V |
| $P_{\rm coupler}$ | 2.0 W |
| $T_e$ | 0.9 eV |
| $f_{pe}$ | 270 MHz |
| $I_{\rm oml}$ | 71.4 mA |
| $I_{\rm dc0}$ | 67.8 mA |

In order to quantitatively compare the degrees of DC current collection enhancement provided by RF signals over a range of frequencies, it appears reasonable to require a fixed power level delivered to the tether sample for all frequencies to be tested.

The experimental system shown on figure 10 was designed in order to dynamically assess the amounts of incident and reflected power on the tested probe in order to control the net power dissipated by the tether in the surrounding plasma. An HP 778D dual directional coupler with a high directivity provides samples of the incident and reflected waves at the source end of the transmission line. The power levels of both samples are measured using two HP 8481A power sensors and two computer-monitored HP 437B digital power meters. An appropriate calibration of the dual di-

rectional coupler, as well as the attenuators, power sensors, and transmission line was performed in order to allow the computer controller (a PC running LabView) to dynamically adjust the amplitude of the input RF signal in order to send a given amount of net power ($P_{\text{probe}} = P_{\text{in}} - P_{\text{out}}$) to the tether sample.

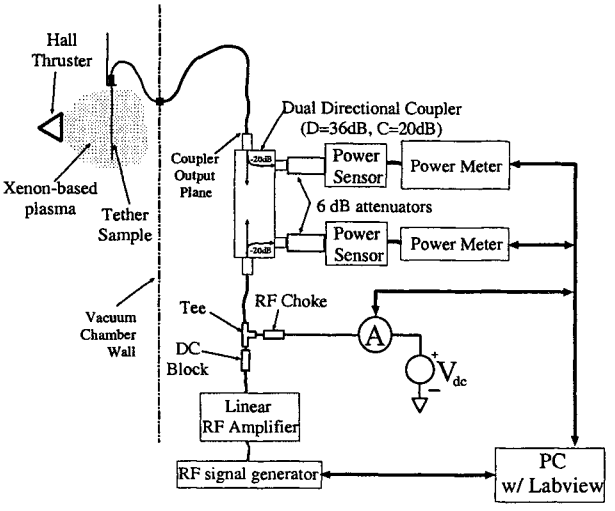


**Fig. 10 Experimental configuration for phase 2 (May 12, 2001)**

In this particular experiment, a 25-W broadband power RF amplifier (ENI 525LA) was used together with a GPIB-capable signal generator (HP ESG-4000A) to provide the RF signal. Unfortunately, in this initial round of tests, an error occured during the calibration of the transmission line running from the output of the coupler to the tether sample inside the vacuum chamber. This error prevented the automated control of the net power dissipated at the tether sample. However, the system still allowed accurate control of the net power at the output plane of the coupler (see Fig. 10).

The results that are shown in Figs. 11 to 15 were obtained by setting a given fixed power (2 W) at the output of the coupler for all signal frequencies. Fig. 12 shows that the output power was indeed kept fairly constant over the frequency range. Fig. 11 gives the variation of the average collected current as a function of frequency under the above-mentioned condition of a fixed net power of 2 W at the output plane of the coupler. It is seen that a maximum current enhancement of approximately 27%, compared to the case without RF power, was achieved near a frequency of 100 MHz, lower than the electron plasma frequency of the plasma (270 MHz).

A correct calibration of the transmission cable was performed after the chamber was vented, in order to recover the actual net power sent. It was thus possible to know, after the fact, what was the actual RF power dissipated in the plasma, eventhough we could not control it directly this time due to the miscalibration

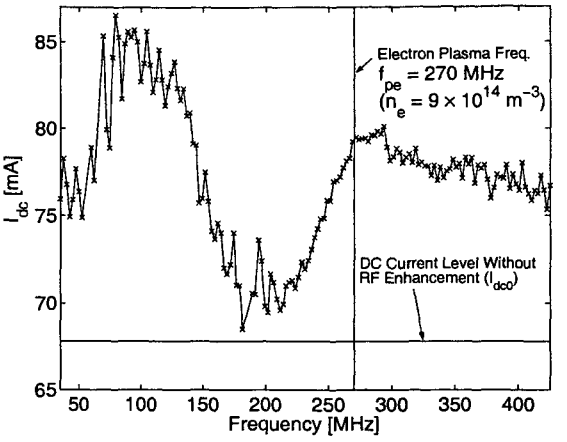


**Fig. 11 Measured average collected current for phase 2.**

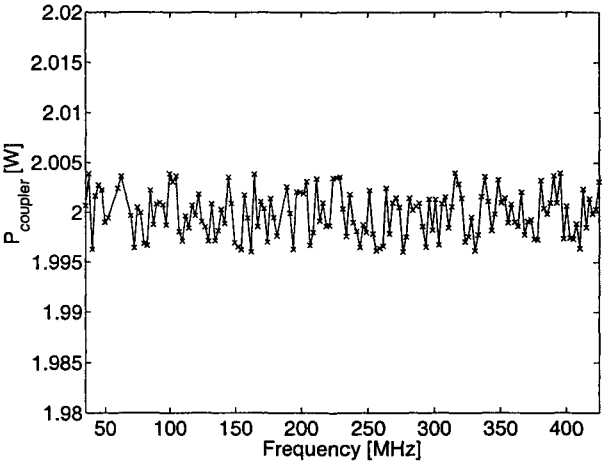


**Fig. 12 Measured net power at the output plane of the dual directional coupler for phase 2.**

issue mentioned above. Fig. 13 shows the measured net power at the probe, accounting for the correct cable calibration. The power values, rather than being fixed at 2 W, fluctuate between 0.6 W and 1.68 W. Those fluctuations are obviously strongly related to the changes in the power reflection coefficient at the probe (Fig. 14), reaching a maximum value near the identified "Resonance" where the power reflection coefficient is at a minimum $\Gamma = 0.066$.

As was done for the analysis of the simulation results in Phase 1 (see figure 9), figure 15 shows the experimental DC current enhancement normalized with the injected RF power measured at the probe, based on the hypothesis that current enhancement depends linearly on the injected power. It is seen that some frequency dependence remains after normalization, with a resonance around 125 MHz and an anti-resonance near 200 MHz, lower than the plasma frequency.

Further measurements are needed, in which the correct calibration for the transmission cable will be used as part of the automated amplitude control scheme in

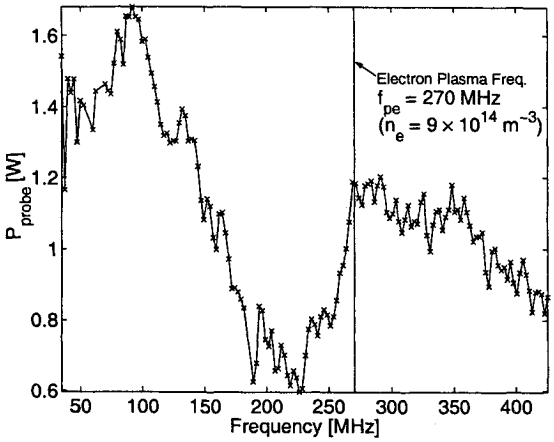


**Fig. 13 Measured net power at the probe for phase 2.**

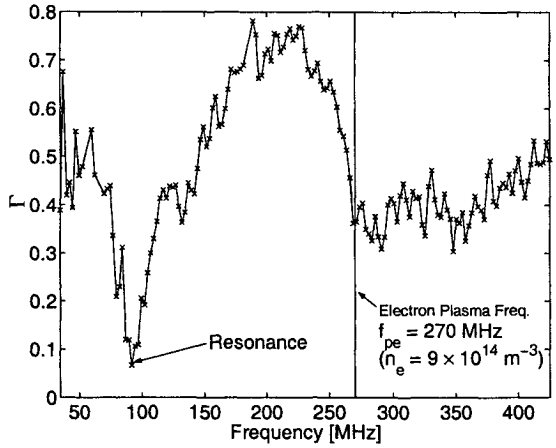


**Fig. 14 Measured power reflection coefficient at the probe for phase 2.**

order to set the net power at the probe to a fixed level for all frequencies. Only then can the true current enhancement variation as a function of frequency be extracted, independent of the impedance variations.

## Conclusions

Initial assessment for the injection of radio frequency power on bare tethers as a means of enhancing electron collection in the OML regime was realized using a PIC 1-d cylindrical model and experimental measurements. Large current enhancements were obtained via simulation at resonance frequencies of the input reactance (i.e., where $X_{\text{in}} = 0$), but at the expense of high RF power. A current enhancement of 750% was observed experimentally (during phase 1 of the tests) for an unknown RF power level.

Since current enhancement is roughly a linear function of the RF input power level, it is better measured with the relative current variation per unit of RF power along a 1-m section of a tether. Using that figure-of-merit, current enhancements up to 9% per meter of tether per RF watt were obtained by simulation at frequencies lower than the resonant frequency (near 90 MHz).

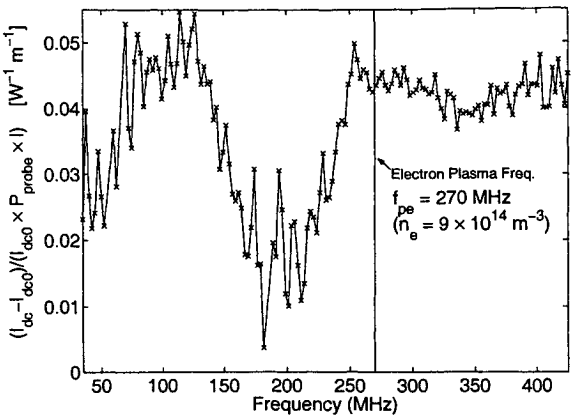


**Fig. 15 Relative DC current enhancement per meter of tether per watt of RF power injected for phase 2.**

In phase 2 of the experimental tests, a new test setup was designed in order to accurately control the power dissipated at the test probe. However, due to calibration issues, the power could only be controlled upstream, at the output of the directional coupler. Current enhancements as high as 27% were observed during that run when 1.68 W of RF power was dissipated at the probe. Normalizing the DC current enhancement with respect to the RF power measured at the probe preserved some of the frequency dependence of the current enhancement.

Further investigations should include a repeat of the experiment performed in phase 2, using the correct calibration for the transmission line in order to gain full control over the RF power sent to the probe. This will provide us with a better understanding of the frequency dependence, if any, of the DC current collection enhancement for a given amount of RF power. A better characterization of the dependence of the enhancement on RF power is also needed.

## Acknowledgments

The authors would like to thank Prof. A. Gallimore for use of the Large Vacuum Test Facility, the PEPL research group (in particular, Travis Patrick, Dan Herman and Tim Smith) for help in performing the experiments as well as Dr. V. Liepa for the loan of several Radio Frequency sources. Finally, É.C. acknowledges the scholarship support of the Natural Sciences and Engineering Research Council of Canada as well as the Communications Research Centre Canada.

## References

[1]Sanmartín, J. R., and Estes, R. D., "The Orbital-Motion-Limited Regime of Cylindrical Langmuir Probes," *Physics of Plasmas*, Vol. 6, No. 1, 1999, pp. 395–405.

[2]Bilén, S. G., Gilchrist, B. E., Bonifazi, C., and Melchioni, E., "Transient Response of an Electrodynamic Tether System in

the Ionosphere: TSS–1 First Results," *Radio Science*, Vol. 30, No. 5, 1995, pp. 1519–1535.

[3]Lepechinsky, D., "La Sonde à Résonance," *L'onde Électrique*, 1965, pp. 1480–1485.

[4]Verboncoeur, J. P., Alves, M. V., Vahedi, V., and Birdsall, C. K., "Simultaneous Potential and Circuit Solution for 1D Bounded Plasma Particle Simulation Codes," *Journal of Computational Physics*, Vol. 104, 1993, pp. 321–328.

[5]Bilén, S. G., and Gilchrist, B. E., "Transient Plasma Sheath Model for Thin Conductors Excited by Negative High Voltages with Application to Electrodynamic Tethers," *IEEE Trans. Plasma Sci.*, Vol. 26, No. 6, 2000, pp. 2058–2074.

[6]Lieberman, Michael A., and Lichtenberg, Allan J., *Principles of Plasma Discharges and Materials Processing*, John Wiley & Sons, 1994.

[7]Haas, James M., Gulczinski III, Frank S., Gallimore, Alec D., Spanjers, Gregory G., and Spores, Ronald A., "Performance Characteristics of a 5 kW Laboratory Hall Thruster," *AIAA Paper AIAA–98–3503*, 1998.

[8]Gilchrist, B. E., Bilén, Sven G., Patrick, Travis A., and Van Noord, Jonathan L., "Bare Electrodynamic Tether Ground Simulations in a Dense, High-Speed Plasma Flow," *AIAA Paper AIAA–2000–3869*, 2000.

[9]Gilchrist, B. E., Bilén, Sven G., and Gallimore, Alec D., "Current Collection to Long, Thin Probes in a Dense High-Speed Flowing Plasma," *2001 Space Technology & Applications International Forum*, 2001.

[10]Onishi, T., Martinez-Sanchez, M., and Cooke, D. L., "Computation of Current to a Moving Bare Tether," in *Proceedings of the 26th International Electric Propulsion Conference*, paper *IEPC99–217*, 1999.